

State-of-Health Aware Optimal Control of Plug-in Electric Vehicles

Yanzhi Wang, Siyu Yue, and Massoud Pedram

Department of Electrical Engineering
University of Southern California, Los Angeles, CA, USA
{yanzhiwa, siyuyue, pedram}@usc.edu

Abstract—Plug-in electric vehicles (PEVs) are key new energy technology to reduce the fossil fuel usage and therefore environmental pollution. The vehicle-to-grid (V2G) technology in the smart grid infrastructure can exploit the electrical energy storage ability of PEV batteries to enhance the stability and reduce peak power demand of the power grid. Through V2G, PEV owners can reduce cost through properly scheduling PEV charging (and perhaps discharging at some time) and at the same time mitigate the negative impacts on the grid. However, there are challenges with V2G services because it is not clear how much PEV battery aging, and therefore also the associated warranty, are affected during V2G operation.

This paper addresses the problem of PEV charging under dynamic pricing, taking into account the degradation of battery state-of-health (SoH) during V2G operations. The objective function to minimize therefore becomes the summation of the energy during PEV charging (and perhaps discharging at some moment) and the extra cost associated with the aging of PEV battery. An optimal algorithm of PEV battery charging is derived to minimize the objective function based on convex optimization techniques. Moreover, this algorithm also accurately accounts for the power loss during charging/discharging of PEV batteries and in power conversion circuitries, which is often neglected in the reference work.

Experimental results demonstrate that the proposed charging control algorithm is able to minimize the combination of electricity cost and battery aging cost, whereas a naive algorithm which only consider the electricity cost may result in as high as 9X battery aging rate.

I. INTRODUCTION

The increasing demands for energy resources all around the world as well as the growing public concern over the environmental impacts of fossil fuels have sparked great interest in renewable energy. Plug-in electric vehicles (PEVs), which utilize electric motors for propulsion, differ from fossil fuel powered vehicles in that the electricity they consume can be generated from a wide range of energy resources, including fossil fuels, nuclear power and renewable energy such as wind energy, solar energy and tidal energy. The battery storage in a PEV can be flexibly recharged on a car park, corporate or public, or at home. Therefore, switching from fossil fuel powered vehicles to PEVs will be a promising solution to the energy crisis and environmental pollution [1].

As more and more PEVs are being plugged into the power grid, the control or management issue of PEV charging arises, since mass unregulated charging of PEVs may result in degradation of power quality and damage utility equipments and customer appliances [2], [3]. Typically, a vehicle aggregator is required to decide the control sequences of a

groups of PEVs based on technical constraints (e.g., the state-of-charge (SoC)) of a PEV) and specific objectives (e.g., minimizing the cost of charging.) A group of previous work [4]-[6] discussed about coordinating PEV group charging in an aggregator in order to minimize power loss in the distribution network, to avoid peak power demand from the grid, and so on.

In the smart grid infrastructure, utility companies could employ real-time or time-of-day *dynamic pricing* techniques (with cheaper rate in the off-peak hours) that incentivize electric devices to shift their load demands from peak hours to off-peak hours [7]-[9]. Moreover, as most of the vehicles are parked on an average of 96% of the time [2], the concept of vehicle-to-grid (V2G) is proposed, where the electrical energy storage ability of PEV batteries is exploited for frequency regulation, load balancing, etc [2], [11], [12]. Through V2G, PEV owners can reduce cost through properly scheduling the charging (or perhaps discharging at some time) of their cars and at the same time mitigate the negative impacts on the grid, i.e., performing valley filling or grid frequency regulation [11], [13]. However, there are challenges with V2G services because it is not clear how much PEV battery aging, and therefore also the associated warranty, are affected during V2G operation. Without a careful consideration of PEV battery aging, the benefits from V2G operation can hardly be realized.

In this paper, we consider the problem of PEV charging under dynamic pricing, with a given departure time and a given target state-of-charge (SoC) level at that time. In this problem, we explicitly take into account the degradation of battery state-of-health (SoH), which is defined as the ratio of the full charge capacity of an aged battery to its designed (nominal) capacity, during V2G operations based on an accurate SoH model. The objective function to minimize therefore becomes the summation of the energy cost during PEV charging (and perhaps discharging at some moment) and the extra cost associated with the aging of PEV battery. We derive an optimal control algorithm of PEV battery charging, which could be implemented in either individual PEVs or in the aggregator, to minimize the objective function based on convex optimization techniques. Moreover, in this algorithm, we also accurately account for the power loss during the charging and discharging process of PEV batteries (e.g., the *rate capacity effect* [22]) and in power conversion circuitries, which is often neglected in the reference work.

The organization of this paper is as follows: Section II describes the power loss modeling of the PHEV storage system, whereas Section III presents the SoH degradation modeling. In Section IV, we provide the formulation and solution of the

optimal PEV battery charging algorithm. Section V presents experimental results, and Section VI concludes the paper.

II. THE PHEV STORAGE MODEL

The most significant portion of power loss in the storage system in a PHEV, which is typically made of NiMH batteries, or Li-ion batteries, is due to the rate capacity effect. To be more specific, high battery discharging current will reduce the amount of available energy that can be extracted from the battery, thereby reducing the battery life [22]. In other words, high-peak pulsed discharging current will deplete much more of the battery's stored energy than a smooth workload with the same total energy demand. We use *discharging efficiency* of a battery to denote the ratio of the battery's output current to the degradation rate of its stored charge. Then the rate capacity effect specifies the fact that the discharging efficiency of a battery decreases with the increase of the battery's discharging current. The rate capacity effect also affects the energy loss in the battery during the charging process in a similar way.

The rate capacity effect can be captured using the Peukert's formula, an empirical formula specifying the battery charging and discharging efficiencies as functions of the charging current I_c and the discharging current I_d , respectively:

$$\eta_{rate,c}(I_c) = \frac{1}{(I_c/I_{ref})^{\alpha_c}}, \quad \eta_{rate,d}(I_d) = \frac{1}{(I_d/I_{ref})^{\alpha_d}} \quad (1)$$

where α_c and α_d are Peukert's coefficients, and their values are typically in the range of 0.1 - 0.3; I_{ref} denotes the *reference current* of the battery, which is proportional to the battery's nominal capacity C_{full} .

We name I_c/I_{ref} and I_d/I_{ref} the battery's *normalized charging current* and *normalized discharging current*, respectively. One can notice that the efficiency values $\eta_{rate,c}(I_c)$ and $\eta_{rate,d}(I_d)$ in Eqn. (1) are greater than 100% if the magnitude of the normalized charging or discharging current is less than one, which implies that the above-mentioned Peukert's formula is not accurate in this case. We modify the Peukert's formula such that the efficiency values $\eta_{rate,c}(I_c)$ and $\eta_{rate,d}(I_d)$ become 100% if the magnitude of the normalized charging/discharging current is less than one. In other words, the battery suffers from no rate capacity effect in this case.

We denote the increase/decrease rate of storage energy by $P_{bat,int}$, which may be positive (charging), negative (discharging), or zero. Based on the modified Peukert's formula, the relation between $P_{bat,int}$ and the storage output power P_{bat} is characterized by

$$P_{bat} = \begin{cases} V_{bat} \cdot I_{bat,ref} \cdot \left(\frac{P_{bat,int}}{V_{bat} \cdot I_{bat,ref}} \right)^{\beta_1}, & \text{if } \frac{P_{bat,int}}{V_{bat} \cdot I_{bat,ref}} > 1 \\ P_{bat,int}, & \text{if } -1 \leq \frac{P_{bat,int}}{V_{bat} \cdot I_{bat,ref}} \leq 1 \\ -V_{bat} \cdot I_{bat,ref} \cdot \left(\frac{|P_{bat,int}|}{V_{bat} \cdot I_{bat,ref}} \right)^{\beta_2}, & \text{if } \frac{P_{bat,int}}{V_{bat} \cdot I_{bat,ref}} < -1 \end{cases} \quad (2)$$

where V_{bat} is the storage terminal voltage and is supposed to be (near-)constant; $I_{bat,ref}$ is the reference current of the battery storage system, which is proportional to its nominal capacity C_{full} given in Ah; coefficient $\beta_1 = 1 + \alpha_c$ is in the range of 1.1 - 1.3, and coefficient $\beta_2 = 1/(1 + \alpha_d)$ is in the range of 0.8 - 0.9.

One can observe that when the storage discharging (or charging) current is the same, the discharging (or charging) efficiency becomes higher (i.e., the rate capacity effect becomes less significant) when the nominal capacity of the storage system is larger.

We use function $P_{bat} = f_{bat}(P_{bat,int})$ to denote the relationship between P_{bat} and $P_{bat,int}$. One important observation is that such function is a convex and monotonically increasing function over the input domain $-\infty < P_{bat,int} < \infty$, as shown in Figure 1.

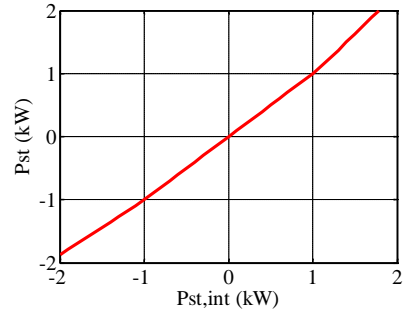


Figure 1. Relationship between P_{bat} and $P_{bat,int}$ of a Li-ion battery.

III. SOH DEGRADATION MODEL

First, we formally define the SoC and SoH degradation of a battery storage bank. The SoC of a battery (bank) is defined by:

$$SoC = \frac{C_{bat}}{C_{full}} \times 100\% \quad (3)$$

where C_{bat} is the amount of charge stored in the battery bank, and C_{full} is the amount of charge in the battery when it is fully charged. The C_{full} value gradually decreases during battery aging (i.e., SoH degradation.) The amount of SoH degradation, denoted by D_{SoH} , is defined as follows:

$$D_{SoH} = \frac{C_{full}^{nom} - C_{full}}{C_{full}^{nom}} \times 100\% \quad (4)$$

where C_{full}^{nom} is nominal value of C_{full} for a fresh new battery.

The SoH of batteries is difficult to estimate because it is related to capacity fading effect (i.e., SoH degradation) that is a result of long-term electrochemical reaction. The capacity fading is related to the carrier concentration loss and internal impedance growth in the batteries. These effects strongly depend on the operating condition of the battery such as charging and discharging current, number of cycles, SoC swing, average SoC, and operation temperature [15], [16]. The characterization of battery cell requires time-consuming experiments. Therefore, mathematical models help us to reduce the time complexity in estimating the SoH degradation. Electrochemistry-based models [17], [18] are generally accurate but not easy to implement. Hence, we apply the SoH

degradation model of Li-ion batteries proposed in [14], which can be applied to cycled charging and discharging of the battery elements and shows a good match with real data.

The SoH degradation model estimates the SoH degradation for cycled charging/discharging of a Li-ion battery cell, where a (charging/discharging) *cycle* is defined as a charging process of the battery cell from SoC_{low} to SoC_{high} and a discharging process right after it from SoC_{high} to SoC_{low} . The SoH degradation during one cycle depends on the *average SoC level* SoC_{avg} and the *SoC swing* SoC_{swing} . We calculate SoC_{avg} and SoC_{swing} of one cycle using:

$$SoC_{avg} = (SoC_{low} + SoC_{high})/2 \quad (5)$$

$$SoC_{swing} = SoC_{high} - SoC_{low} \quad (6)$$

SoC_{swing} achieves the maximum value of 1.0 (100%) for the full 100% depth of discharge cycle, i.e., the SoC ranges from 0 up to 100% and back to 0.

The SoH degradation $D_{SoH,cycle}$ during this charging/discharging cycle, accounting for both average SoC level and SoC swing, is:

$$\begin{aligned} D_1 &= K_{co} \cdot \exp \left[(SoC_{swing} - 1) \cdot \frac{T_{ref}}{K_{ex} \cdot T_B} \right] + 0.2 \frac{\tau}{\tau_{life}} \\ D_2 &= D_1 \cdot \exp [4K_{SoC} \cdot (SoC_{avg} - 0.5)] \cdot (1 - D_{SoH}) \\ D_{SoH,cycle} &= D_2 \cdot \exp \left[K_T \cdot (T_B - T_{ref}) \cdot \frac{T_{ref}}{T_B} \right] \end{aligned} \quad (7)$$

where K_{co} , K_{ex} , K_{SoC} , and K_T are battery specific parameters; T_B and T_{ref} are the operation battery temperature and reference battery temperature, respectively; τ is the duration of this charging/discharging cycle; τ_{life} is the calendar life of the battery. We use $D_{SoH,cycle}(SoC_{swing}, SoC_{avg})$ to denote the relationship between $D_{SoH,cycle}$, SoC_{swing} , and SoC_{avg} . The total SoH degradation (from a new battery) after M charging and discharging cycles is calculated by:

$$D_{SoH} = \sum_{m=1}^M D_{SoH,cycle,m} \quad (8)$$

where $D_{SoH,cycle,m}$ denotes the SoH degradation in the m^{th} cycle.

In Eqn. (8), the normalized SoH degradation value D_{SoH} increases over the battery lifetime from 0 (brand new) to 100% (no capacity left). Typically, the values of $D_{SoH} = 20\%$ or $D_{SoH} = 30\%$, which indicate 80% or 70% remaining capacity, respectively, are used in literature to measure the battery's end of life. The relationship between the Li-ion battery SoH degradation versus the SoC swing and average SoC level is shown in Figure 2. In this experiment, we change the duration of a cycle to achieve different average SoC levels and SoC swings. We repeat the charge and discharge cycling until the battery reaches $D_{SoH} = 20\%$, and record the total number of cycles (i.e., the *cycle life* of the battery.) The results are shown in Figure 2. There are two important observations: (i) a higher SoH degradation rate is caused by both higher SoC swing and higher average SoC level in each charging/discharging cycle, (ii) the cycle life of a Li-ion battery increases superlinearly

with respect to the reduction of SoC swing and average SoC. We make use of these observations as well as the function $D_{SoH,cycle}(SoC_{swing}, SoC_{avg})$ in the rest of this paper.

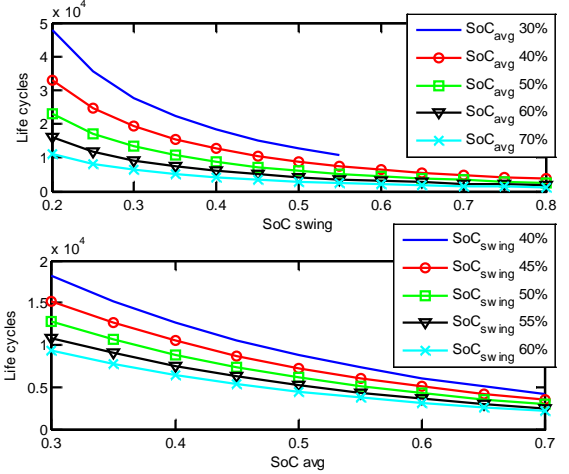


Figure 2. Li-ion battery SoH degradation versus SoC swing (at different average SoC levels) and average SoC level (at different SoC swings).

IV. PROBLEM FORMULATION AND OPTIMIZATION

In this section, we present the formulation and solution of the optimal PEV battery charging problem under *time-of-day* pricing. We consider a *slotted time* model, i.e., all system constraints as well as decisions are provided for discrete time intervals of equal and constant length Δ_T . The PEV begins parking at home or at a public parking lot at the beginning of the 1st time slot, and it is scheduled to depart at the end of time slot N . The initial SoC level of the PEV battery is given by $SoC[0] = SoC_{ini}$, and the target SoC level is SoC_{tar} when the PEV departs. We consider the time-of-day energy pricing function $Price[i]$ for $1 \leq i \leq N$ over all N time slots, which is pre-announced by the utility company before PEV charging. Let $P_{bat}[i]$ for $1 \leq i \leq N$ denote the battery charging/discharging power in each time slot, where $P_{bat}[i] > 0$ implies charging and $P_{bat}[i] < 0$ implies discharging. Let $P_{bat,int}[i]$ for $1 \leq i \leq N$ denote the energy accumulation/decrease rate in the PEV battery. We have $P_{bat}[i] = f_{bat}(P_{bat,int}[i])$ as in equation (2). The PEV charging controller, which resides either in individual vehicles or in an aggregator, controls the battery charging/discharging power $P_{bat}[i]$ for $1 \leq i \leq N$.

The objective function to minimize is comprised of two parts: the energy cost during PEV charging (and perhaps discharging at some moments) and the cost associated with PEV battery aging, as shown below:

$$Cost_{total} = Cost_{energy} + Cost_{aging} \quad (9)$$

The energy cost in Eqn. (9) is given by the following equation:

$$\begin{aligned} Cost_{energy} &= \sum_{i=1}^N Price[i] \cdot \Delta_T \cdot \\ &\left\{ \frac{1}{\eta_c} P_{bat}[i] \cdot \mathbf{I}[P_{bat}[i] > 0] + \eta_d P_{bat}[i] \cdot \mathbf{I}[P_{bat}[i] < 0] \right\} \end{aligned} \quad (10)$$

where $\eta_c, \eta_d < 1$ are the charging and discharging efficiency of the AC/DC power conversion circuitry between the PEV battery and grid, and $\mathbf{I}[-]$ is the indicator function.

To calculate $Cost_{aging}$, we provide as follows an estimate of the SoH degradation of the PEV battery during the charging process and the previous driving period. We approximate the combination of the driving period and charging process as multiple discharge/charge cycles of PEV battery. During the driving period, the SoC drops from SoC_{tar} (suppose that the SoC level at the beginning of the previous driving period is also SoC_{tar}) to SoC_{ini} . Therefore the highest and lowest SoC value SoC_{low} in this discharge/charge cycle is:

$$\begin{aligned} SoC_{high} &= \max_{0 \leq i \leq N} SoC[i] \\ SoC_{low} &= \min_{0 \leq i \leq N} SoC[i] \end{aligned} \quad (11)$$

where $SoC[i]$ denotes the SoC value at the end of time slot i ($SoC[0] = SoC_{ini}$), and is calculated by:

$$SoC[i] = SoC[0] + \sum_{j=1}^i \frac{P_{bat,int}[j] \cdot \Delta_T}{V_{bat} \cdot C_{full}} \quad (12)$$

The number of cycles during the combination of driving period and charging process is:

$$N_c = \sum_{j=1}^N \frac{P_{bat,int}[j] \cdot \mathbf{I}[P_{bat}[j] > 0] \cdot \Delta_T}{V_{bat} \cdot C_{full} \cdot (SoC_{swing})} \quad (13)$$

where $SoC_{swing} = SoC_{high} - SoC_{low}$. Finally, the cost associated with SoH degradation of the PEV battery is given by (we assume that the battery reaches end-of-life when SoH degradation is 30%):

$$Cost_{aging} = \frac{D_{SoH,cycle}(SoC_{swing}, SoC_{avg}) \cdot N_c}{0.3} \cdot Cost_{bat} \quad (14)$$

where $Cost_{bat}$ is the cost to purchase the PEV battery (The state-of-art Li-ion battery capital cost is between \$200 to \$500 per kWh [20]); $SoC_{avg} = \frac{SoC_{high} + SoC_{low}}{2}$; and function $D_{SoH,cycle}(SoC_{swing}, SoC_{avg})$ is defined in Section III.

We formally describe the PEV battery charging problem as follows:

Given: Initial SoC SoC_{ini} , target SoC SoC_{tar} , time-of-day energy pricing function $Price[i]$ for $1 \leq i \leq N$.

Find: Battery charging/discharging current profile $P_{bat}[i]$ for $1 \leq i \leq N$.

Optimize: Objective function Eqn. (9).

Subject to:

Constraints on the maximum charging/discharging power:

$$-P_{MAX,d} \leq P_{bat}[i] \leq P_{MAX,c}, \forall i \quad (15)$$

Constraints on the SoC levels:

$$0 \leq SoC[i] \leq 1, \forall i \quad (16)$$

Satisfying the final target SoC level:

$$SoC[N] \geq SoC_{tar} \quad (17)$$

We present the optimal solution of the PEV battery charging problem. The motivation of the optimal solution is that $D_{SoH,cycle}(SoC_{swing}, SoC_{avg})$ only depends on SoC_{low} and SoC_{high} . The optimal solution is comprised of an outer loop and a kernel problem. In the outer loop, we perform parameter sweeping on SoC_{low} and SoC_{high} . With given SoC_{low} and SoC_{high} , the kernel problem is an optimization problem to find the battery charging/discharging profile with regard to an additional constraint on $SoC[i]$:

$$SoC_{low} \leq SoC[i] \leq SoC_{high}, \forall i \quad (18)$$

In order to solve the kernel problem optimally and efficiently, we use $P_{bat,int}[i]$ for $1 \leq i \leq N$ as the optimization variables since it can help transform the kernel problem into a standard convex optimization problem. Please note that in reality the PEV charging controller still controls $P_{bat}[i]$ for $1 \leq i \leq N$.

We observe from (10) that $Cost_{energy}$ is a convex and increasing function of $P_{bat}[i]$ for $1 \leq i \leq N$. We know from Section II that $P_{bat} = f_{bat}(P_{bat,int})$ is a convex function. Therefore, $Cost_{energy}$ is a convex function of the optimization variables $P_{bat,int}[i]$ for $1 \leq i \leq N$ according to the rules of convexity in function composition [23]. As for $Cost_{aging}$, it is also a convex function of $P_{bat,int}[i]$ for $1 \leq i \leq N$. Moreover, the constraints of the kernel problem are all linear inequality constraints, e.g., (15) of the optimization variables because $SoC[i]$ is a linear function of $P_{bat,int}[i]$ for $1 \leq i \leq N$. Based on the above observations, we conclude that the kernel problem is a standard convex optimization problem with convex objective functions and linear constraints. Hence, it can be optimally solved using standard optimization tools with polynomial time complexity [23]. Therefore, the optimal solution for the complete problem has pseudo polynomial time complexity,

V. EXPERIMENTAL RESULTS

In the simulation, we consider a 24kWh Li-ion battery, and a charging period of 12 hours, divided into 24 time slots. We compare with two baseline solutions. The first baseline solution is one which neglects the aging cost and only minimize the energy cost (denoted by MEC). The second baseline solution considers aging cost but does not sell back electricity (denoted by NSB).

First we use a pricing function as shown in Figure 3(a). The pricing function consists of two low-price sections and two high-price sections. TABLE I shows the energy cost and aging cost of the optimal solution for different low and high electricity unit prices, and different Li-ion battery prices. It also shows the energy cost and aging cost of MEC and NSB solutions. A negative energy cost indicates the EV makes some profit by buying electricity when the electricity price is low and selling back when the price is high, at the cost of exacerbating the aging process of the battery. As shown in TABLE I, although MEC solution makes the most profit by selling back

TABLE I. SIMULATION RESULTS

Electricity Price(\$/kWh)		Li-ion Price (\$/kWh)	Optimal Solution (\$)			Minimum Energy Cost Solution (\$)			No Selling Back Solution (\$)		
Low	High		Energy Cost	Aging Cost	Total	Energy Cost	Aging Cost	Total	Energy Cost	Aging Cost	Total
0.1	0.2	200	0.750	0.795	1.545	0.365	2.092	2.457	0.750	0.795	1.545
0.1	0.2	500	0.750	1.986	2.736	0.365	5.230	5.595	0.750	1.986	2.736
0.1	0.3	200	-0.136	1.478	1.342	-2.212	7.092	4.880	0.750	0.795	1.545
0.1	0.3	500	0.750	1.986	2.736	-2.212	17.731	15.52	0.750	1.986	2.736
0.1	0.4	200	-2.424	2.649	0.225	-4.827	7.092	2.265	0.750	0.795	1.545
0.1	0.4	500	0.750	1.986	2.736	-4.827	17.731	12.90	0.750	1.986	2.736
0.1	0.5	200	-5.406	3.932	-1.47	-7.442	7.092	-0.35	0.750	0.795	1.545
0.1	0.5	500	0.663	2.053	2.716	-7.442	17.731	10.29	0.750	1.986	2.736

electric energy, it results in significant aging cost. In some of the test cases, the aging cost, or equivalently, the aging rate of MEC solution is almost 9X as large as that of the optimal solution. Nonetheless, both solutions will maximize the amount of energy sold back to the grid when the electricity price difference is large and the price of Li-ion battery is low. On the other hand, NSB solution achieves the minimum aging cost, but has the largest energy cost of the three. Figure 3(b) shows the charging/discharging profile of all three solutions for the case where high electricity price is \$0.3/kWh and Li-ion battery price is \$200/kWh. As shown in the figure, MEC solution uses the most of the battery.

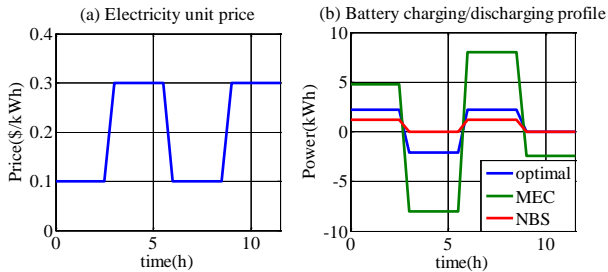


Figure 3. (a) Electricity price; (b) Battery charging/discharging profile.

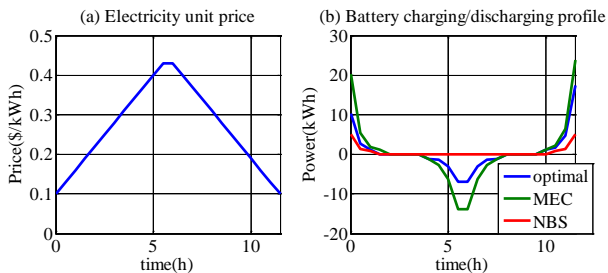


Figure 4. Electricity price and battery charging/discharging profile of a different test case.

Figure 4 shows the electricity price vector and the battery charging/discharging profile of a different test case. Although the electricity price at the first and last time slots are the cheapest, all solutions charge the battery at some other time slots as well since the charging efficiency at the first and last time slots are much lower due to the rate capacity effect. The total cost achieved by the optimal solution (1.15) is 68% less than MEC solution (3.59) and 37% less than the NSB solution (1.82).

VI. CONCLUSION

In this paper, we consider the problem of PEV charging under dynamic pricing, with a given departure time and a given

target SoC level at that time. In this problem, we explicitly take into consideration the degradation of battery SoH during V2G operations, based on an accurate SoH modeling. The objective function to minimize therefore becomes the summation of the energy cost during PEV charging (and perhaps discharging at some moment) and the extra cost associated with the aging of PEV battery. We derive an optimal control algorithm of PEV battery charging, which could be implemented in either individual PEVs or in the aggregator, to minimize the objective function based on convex optimization techniques. Moreover, the proposed algorithm also accurately accounts for the power loss during the charging and discharging process of PEV batteries, especially the rate capacity effect, and in power conversion circuits, which is often neglected in the reference work.

Experimental results demonstrate that the proposed optimal PEV charging algorithm minimizes the combination of electricity cost and battery aging cost and achieves much smaller Li-ion battery aging rate.

ACKNOWLEDGEMENT

This work is supported by the Software and Hardware Foundations program of the NSF's Directorate for Computer & Information Science & Engineering.

REFERENCES

- [1] C. C. Chan, "An overview of electric vehicles technology," *Proceedings of the IEEE*, vol. 81, pp. 1202 - 1213, Sep. 1993.
- [2] A. Ipakchi and F. Albuyeh, "Grid of the future," *IEEE Power and Energy Magazine*, vol. 7, no. 2, pp. 52 - 62, 2009.
- [3] R. Liu, L. Dow, and E. Liu, "A survey of PEV impacts on electric utilities," in *Proc. of IEEE Innovative Smart Grid Technologies (ISGT)*, 2011, pp. 1 - 8.
- [4] K. Shimizu, T. Masuta, Y. Ota, and A. Yokoyama, "Load frequency control in power system using vehicle-to-grid system considering the customer convenience of electric vehicles," in *International Conf. Power System Technology*, 2010, pp. 1 - 8.
- [5] S. Han, S. Han, and K. Sezaki, "Optimal control of the plug-in electric vehicles for V2G frequency regulation using quadratic programming," in *IEEE PES Innovative Smart Grid Technologies (ISGT)*, 2011, pp. 1 - 6.
- [6] C.-T. Li, C. Ahn, H. Peng, and J. Sun, "Integration of plug-in electric vehicles charging and wind energy scheduling on electricity grid," in *IEEE PES Innovative Smart Grid Technologies (ISGT)*, 2012, pp. 1 - 7.
- [7] X. Fang, S. Misra, G. Xue, and D. Yang, "Smart grid - the new and improved power grid: a survey," *IEEE Communications Surveys & Tutorials*, vol. 14, pp. 944 - 980, Fourth Quarter 2012.
- [8] S. Kishore and L. V. Snyder, "Control mechanisms for residential electricity demand in SmartGrids," *IEEE SmartGridComm*, 2010.
- [9] S. Caron and G. Kesidis, "Incentive-based energy consumption scheduling algorithms for the Smart Grid," *Proc. of IEEE SmartGridComm*, 2010.

- [10] W. Kempton and J. Tomic, "Vehicle-to-grid power implementation: from stabilizing the grid to supporting large-scale renewable energy," *Journal of Power Sources*, vol. 144, pp. 280 - 294, Jun. 2005.
- [11] J. Tomic and W. Kempton, "Using fleets of electric-drive vehicles for grid support," *Journal of Power Sources*, vol. 168, pp. 459 - 468, Jun. 2007.
- [12] C. Guille and G. Gross, "Design of a concept framework for the V2G implementation," in *IEEE Energy2030 Conference*, 2008, pp. 1 - 3.
- [13] C. Wu, H. Mohsenian-Rad, and J. Huang, "Vehicle-to-aggregator interaction game," *IEEE Transactions on Smart Grid*, vol. 3, no. 1, March 2012.
- [14] A. Millner, "Modeling Lithium Ion battery degradation in electric vehicles," *IEEE Conference on Innovative Technologies for an Efficient and Reliable Electricity Supply (CITRES)*, 2010.
- [15] M. Dubbary, V. Svoboda, R. Hwu, and B. Liaw, "Capacity and power fading mechanism identification from a commercial cell evaluation," *Journal of Power Sources*, 2007.
- [16] S. Peterson, J. Apt, and Whitacre, "Lithium-ion battery cell degradation resulting from realistic vehicle and vehicle-to-grid utilization," *Journal of Power Sources*, 2010.
- [17] Q. Zhang and R. White, "Capacity fade analysis of a lithium ion cell," *Journal of Power Sources*, 2008.
- [18] P. Rong and M. Pedram, "An analytical model for predicting the remaining battery capacity of Lithium-ion batteries," *IEEE Trans. on VLSI Systems*, 2006.
- [19] Q. Xie, X. Lin, Y. Wang, M. Pedram, D. Shin, and N. Chang, "State of health aware charge management in hybrid electrical energy storage systems," in *Design, Automation, and Test in Europe (DATE)*, 2012.
- [20] D. Zhu, Y. Wang, S. Yue, Q. Xie, N. Chang, and M. Pedram, "Maximizing return on investment of a grid-connected hybrid electrical energy storage system," in *Asia and South Pacific Design Automation Conference (ASP-DAC)*, 2013.
- [21] M. Pedram, N. Chang, Y. Kim, and Y. Wang, "Hybrid electrical storage systems," in *International Symposium on Low Power Electronics Design (ISLPED)*, 2011.
- [22] D. Linden and T. B. Reddy, *Handbook of Batteries*, McGraw-Hill Professional, 2001.
- [23] S. Boyd and L. Vandenberghe, *Convex Optimization*, Cambridge University Press, 2004.